THE ASTROPHYSICAL JOURNAL, 616:L1–L6, 2004 November 20

THE SUBMILLIMETER ARRAY

PAUL T. P. HO
Harvard-Smithsonian Center for Astrophysics, 60 Garden Street, Cambridge, MA 02138; and Academia Sinica Institute of Astronomy and Astrophysics, P.O. Box 23-141, Taipei 106, Taiwan; ho@cfa.harvard.edu
JAMES M. MORAN
Harvard-Smithsonian Center for Astrophysics, 60 Garden Street, Cambridge, MA 02138; jmmoran@cfa.harvard.edu
AND
KWOK YUNG LO
National Radio Astronomy Observatory, 520 Edgemont Road, Charlottesville, VA 22903; and Academia Sinica Institute of Astronomy and Astrophysics, P.O. Box 23-141, Taipei 106, Taiwan; flo@nrao.edu
Received 2004 May 13; accepted 2004 June 10; published 2004 October 28

ABSTRACT

The Submillimeter Array, a collaborative project of the Smithsonian Astrophysical Observatory and the Academia Sinica Institute of Astronomy and Astrophysics, has begun operation on Mauna Kea in Hawaii. The array comprises a total of eight 6 m telescopes, which will cover the frequency range of 180–900 GHz. All eight telescopes have been deployed and are operational. First scientific results utilizing the three receiver bands at 230, 345, and 690 GHz have been obtained and are presented in the accompanying Letters.

Subject headings: instrumentation: interferometers — submillimeter — telescopes

1. INTRODUCTION

The Submillimeter Array (SMA) Project was conceived at the Smithsonian Astrophysical Observatory (SAO) in 1983 as part of a broad initiative by its new director, Irwin Shapiro, to achieve high-resolution observational capability across a wide range of the electromagnetic spectrum. The aim of the SMA is to use interferometric techniques to explore submillimeter wavelengths with high angular resolution. One measure of the importance of the submillimeter window derives from the fact that the bulk of the visible universe is at a relatively cold temperature of about 10 K, thereby placing the peak of the radiation curve in the submillimeter and far-infrared range. From the ground, the submillimeter wavelengths are as close as we can get to this radiation peak, and high-resolution observations are only possible from the ground until space far-infrared interferometry becomes feasible. Furthermore, many more unique and high-excitation molecular lines become available in the submillimeter window. In the 1980s, only single-aperture instruments such as the 10 m Caltech Submillimeter Observatory (CSO), the 15 m James Clerk Maxwell Telescope (JCMT), the 10 m Heinrich Hertz Submillimeter Telescope, and the 3 m Kolner Observatorium für Submillimeter Astronomie were operating or planning to operate at submillimeter wavelengths. The SMA was designed to increase the available angular resolution by a factor of 30. A formal proposal was presented to the Smithsonian Institution in 1984 (Moran et al. 1984) and was reviewed favorably by the community. Initial funding of the project began with the establishment of a submillimeter-wavelength receiver laboratory at SAO in 1987. Two years later, the design study for the SMA (Masson 1992) was funded, and construction funds followed in 1991. Several sites for the array were considered, including Mount Graham in Arizona, a location near the South Pole, and the Atacama desert in Chile (Raffin & Kusunoki 1992). Mauna Kea in Hawaii was ultimately chosen, in part because of the existence of good infrastructure as well as other programmatic reasons, and in 1994 an agreement was reached with the University of Hawaii for the construction of the array in "Millimeter Valley" adjacent to the CSO and the JCMT at an elevation of 4080 m. This specific location was selected because of the potential for linking up with CSO and JCMT as well as the ability to achieve baselines of at least 500 m without great changes in elevation, with the possibility of even longer baselines in the future.

The initial concept for the SMA was six 6 m telescopes, the parameters of which were driven by (1) the desire for a fast instrument that would sample the UV plane adequately, even for short observations, (2) the desire to have at least the same collecting area as the existing submillimeter telescopes, (3) the desire for a reasonably large primary beam at the highest frequencies in order to make the pointing requirements manageable and the field of view reasonably large, and (4) the balance between the cost of telescopes, which scales faster than the square of the aperture, and the cost of receivers, electronics, and a correlator.

In 1996, the Academia Sinica Institute of Astronomy and Astrophysics (ASIAA) joined the SMA project by agreeing to add two more telescopes and all associated electronics, including a doubling of the correlator. The Academia Sinica agreed with the cost effectiveness of this plan and funded the expansion of the SMA as the first astronomical project at ASIAA. The addition of two elements increased the number of instantaneous baselines from 15 to 28, nearly doubling the speed of the array for some applications. While the addition of a partner introduced complications in the construction process, the power of the SMA and its scientific potential were increased significantly.

SAO personnel designed the telescope, receivers, and electronics. Fabrication of the mount, the reflector panels, and other subsystems was performed by subcontractors, while the assembly was done by SAO staff at the SMA facilities located at the Haystack Observatory in Westford, Massachusetts. After initial tests including holography at 94 GHz and interferometry at 230 GHz, the individual telescopes were disassembled, shipped to Hawaii, and reassembled in the SMA assembly hall on Mauna Kea. The Aeronautical Research Laboratory (ARL) in Taiwan was the primary contractor for fabrication of the two telescopes contributed by ASIAA. By the end of 2003, all eight elements of the SMA had been deployed on top of Mauna Kea, and the SMA was formally dedicated on 2003 November 22.

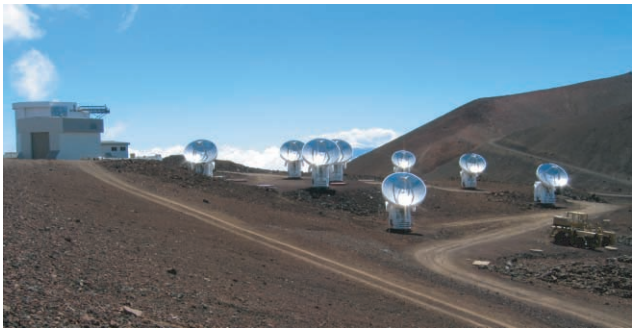

FIG. 1.—View of the SMA in the direction of Mauna Loa. The assembly/maintenance building and attached control building are in the top left. The JCMT can be seen rising above them in the background. The slope of Pu'u Poli'ahu rises in back of the Array on the right side. The transporter used to move the antennas is in the right side of the foreground. In its most compact configuration, all antennas can occupy the flat plateau where four of the antennas sit. At the end of 2003, all eight elements of the SMA were operating on Mauna Kea in Hawaii. R. Blundell and B. Liu headed the antenna groups at SAO and ASIAA/ARL, respectively.

Figure 1 shows the completed SMA in a fairly compact configuration. Table 1 gives the characteristics of the SMA.

TABLE 1

BASIC CHARACTERISTICS OF THE SMA

Components	Specifications
Interferometer elements	Eight 6 m, f/0.4 paraboloids, bent-Nasmyth optics
Telescope mount	Alt-azimuth
Telescope backup structure	Carbon fiber struts, steel nodes, rear cladding
Primary reflector	Four rows of 72 machined cast aluminum panels
Surface accuracy	12 μm rms
Secondary reflector	Machined aluminum, 10 Hz chopping
Array configuration	Four nested rings, 24 pads, up to eight pads per ring
Available baselines	9–500 m
Operating frequencies	180–900 GHz
Maximum angular resolution	0.″5–0.″1
Primary beam field of view	70″–14″
Receiver bands	230, 345, 460, 690, and 850 GHz
Number of receivers	Eight per telescope, two simultaneous bands
Correlator	Hybrid analog-digital, 2 × 28 baselines
Number of spectral channels	172,000
Maximum bandwidth	2 GHz
Maximum spectral resolution	0.06 MHz
Maximum data rate	>10 GB day^{-1} for 1 s integrations

2. DESCRIPTION OF THE INSTRUMENT

2.1. *Construction of the Telescopes*

In 1992, SAO chose to be the general contractor for construction of the telescopes. While submillimeter-wavelength telescopes had already been built by other institutions, the requirements of interferometry presented additional challenges such as the need for exceptional mechanical stability and transportability of the antennas. The massive size of the mount was necessary to provide stability under stringent pointing requirements. The reflector and its backup support structure were designed by P. Raffin and the SAO staff (Raffin 1991a, 1991b). The reflector surface was composed of machined cast aluminum panels, which were chosen over carbon fiber panels because of concerns over conditions on Mauna Kea that can include windblown abrasive volcanic dust and storms that bring heavy snow and thick ice accumulations. In order to achieve the necessary surface accuracy in the manufacturing process as well as good thermal performance in the field, four rows of individual panels, each about 1 m in size, were employed. A mean surface accuracy of 6 μm was achieved for the individual panels. To hold the surface in shape, carbon fiber tubes and steel nodes were used to form an open backup structure. The individual panels were attached to the backup structure via four mechanical adjusters per panel. The surfaces were adjusted from the front, as the backup structures were covered by an aluminum skin in order to protect them from the weather. The adjusters not only held the reflector panels to the backup structure, but because of the over constraint of the four-point support, they allowed twists within each panel to be corrected. The use of carbon fiber tubes provided a lightweight and rigid structure with a very low thermal expansion coefficient. A linear screw drive was chosen to move the telescope in the elevation direction because it allowed for a large, stable walk-in cabin for the receivers. The receiver cabin was built around the mount in between the elevation bearings, and the optics chosen were bent-Nasmyth via a tertiary mirror behind the center of the reflector. This arrangement allowed the receivers to be maintained with a constant gravity vector in order to ensure mechanical stability, which was deemed important for receiver stability.

The telescopes were put together in the SMA assembly hall at the MIT Haystack Observatory in Westford, Massachusetts; the first prototype was built in 1996, and an improved version was put into operation in 1997. Two copies of the second prototype operated successfully as an interferometer at 230 GHz in the fall of 1998 at Haystack. These two telescopes were deployed to Hawaii the following year and obtained first fringes on Mauna Kea in 1999 September: a major milestone for the project. From that point on, the production models of the telescopes began to arrive in Hawaii, incorporating improvements in the receiver cabin, electronics, and servo systems. The final versions of the primary reflectors of the telescope, including the carbon fiber backup structures, were assembled on Mauna Kea using a special rotating template. In the last 4 years, the two telescopes from Taiwan arrived in Hawaii, four more telescopes arrived from Massachusetts, and the original two prototype telescopes were rebuilt in Westford.

2.2. *Holographic Adjustments of the Surface*

The reflectors were assembled with an initial accuracy of about 60 μm. After the reflectors were installed on the telescope mount, holographic alignment was performed with a 232 GHz radiation source mounted on the catwalk of the Subaru Telescope (Sridharan et al. 2004). Located about 200 m from the center of the array at an elevation angle of about 20°, the test signal was observed through the SMA optics with the subreflectors set to their near-field focus positions. The far-field beam response of the telescope under study was measured by scanning it while a second telescope provided the phase reference. Amplitude and phase data were acquired with an on-the-fly technique (i.e., continuous movement of the reflector). Fourier transform of the complex map gave the distribution of illumination (amplitude) and surface deviations (phase). The scanning resolution was 33″, which corresponded to a spatial resolution on the reflector of about 10 cm. The holographic procedure, while simple in concept, had many subtleties. Corrections for the near-field geometry, multiple reflections, and diffraction effects had to be made. The effects of multiple reflections were mitigated by averaging maps with the sub-

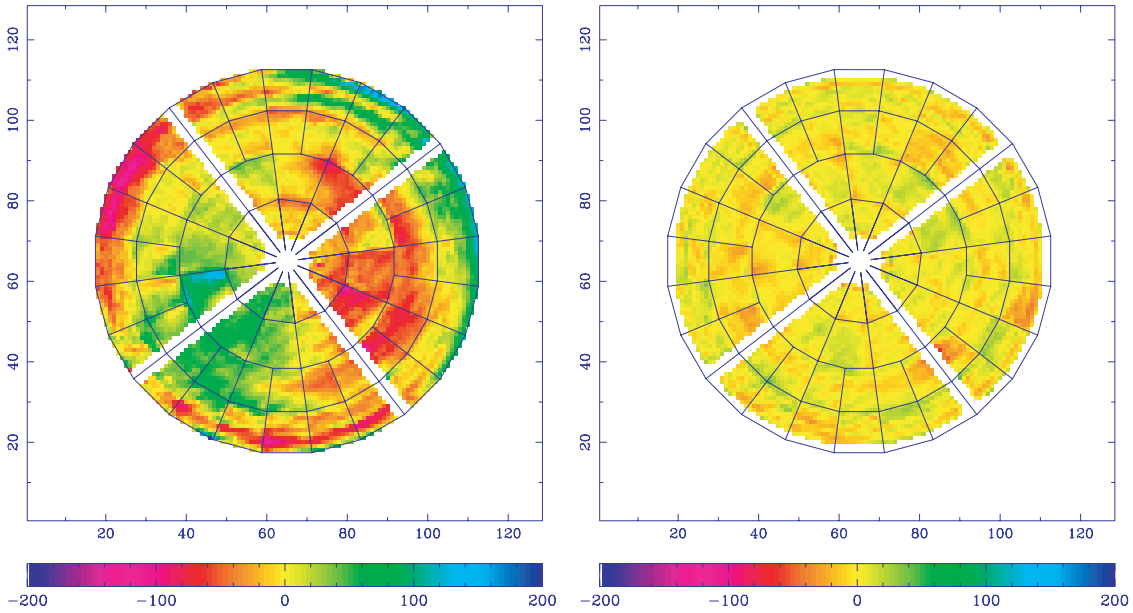

FIG. 2.—Holographic measurements of the surface of Telescope 2, before (*left*) and after (*right*) a series of panel adjustments. The rms accuracy improved from about 65 to about 12 μm. T. K. Sridharan and N. Patel have been leading the efforts to measure and reset the surfaces of all the telescopes.

reflectors in various focus positions. Typically, three or four rounds of holography and resetting of the panels were required to reach the goal of 12 μm accuracy for the surface at an elevation of 20°. Figure 2 shows the deviations in the surface of one of the reflectors before and after the setting of the surface with this holographic technique. The reflector surfaces have been monitored for long-term stability. On the timescale of several months, the surface accuracy appears to be stable at about 11 μm rms. This includes the changes due to redeployment of the telescope from one pad to another. In the future, holography at 682 GHz will be used for more precision, and a celestial holography capability will be developed to enable studies of the reflector behavior under different conditions of gravitational deformation over a wide range of elevation angle.

The surface accuracy also can be checked by measuring the aperture efficiency of the telescope while observing a planet. Initial measurements indicate 70%–75% efficiency at 230 GHz, 50%–60% efficiency at 345 GHz, and about 40% at 680 GHz. Optimization of the surface accuracy of each telescope is continuing.

2.3. *Configuration of the Array*

For an interferometer array with a small number of elements, the configuration is important for achieving the best *u-v* plane coverage and the best image quality. The design of the SMA configuration was driven by the desire for a uniform sampling of *u-v* plane spacings within a circular boundary, whose radius sets the angular resolution. Scaled Y-configurations such as the Very Large Array (VLA) are centrally condensed and undersample the long spacings. The redundancies in such configurations have distinct advantages but compromise the *u-v* plane coverage if the number of elements in the array is small. A configuration based on the Reuleaux triangle, which is an equilateral triangle whose sides have been replaced with circular arcs with the opposite vertices as their centers, was found to provide the most uniform *u-v* plane sampling. By locating the interferometer elements on a curve of constant width such as the Reuleaux triangle, the maximum separation between telescopes is a constant. This ensures that the maximum *u-v* plane spacings lie on a circle, thereby resulting in a circular beam for observations at the zenith. The choice of a triangle, versus a polygon of more sides, ensures that the angles between baseline vectors, and therefore potential differences between projected baselines, are maximized. This results in a more uniform sampling distribution in the *u-v* plane. The sampling of the shorter spacings depends on the actual locations of the array elements on the curves, which was optimized with a neural network search algorithm (Keto 1997). Addition of the two ASIAA telescopes was accommodated within this Reuleaux triangle scheme on an ad hoc basis. The SMA configuration works well for a small number of interferometer elements. For an array with a large number of telescopes, their specific distribution is less critical.

To provide different angular resolutions the array consists of four nested "rings" of 24 pads. Each of the rings is an optimized Reuleaux triangle, accommodating up to eight pads. The rings are nested in order to share some of the pads and thereby reduce costs. Some compromises were eventually made because of the topography of the site. The actual layout of the pads is shown in Figure 3.

Because of the uneven terrain of the SMA as well as environmental restrictions, the telescopes had to be transported without the use of rails as was the case of the VLA. A special transporter was designed to pick up and move the 50 ton telescopes. This piece of equipment drives under its own power and is nimble enough so that several antennas can be repositioned in a day.

2.4. *Receivers and Electronics*

The front end receiver electronics in each antenna are housed in closed cycle helium cryostats (Daikin model CG-308SCPT cryocooler). The cryostats use a two-stage Gifford McMahon system to reach 70 and 15 K, respectively, and a Joule-Thompson valve to reach 4 K. Each cryostat has room for eight receiver inserts and a capacity of 2.5 watts at 4 K (Blundell et al. 1998). An optics cage is mounted above the cryostat, which splits the polarizations of the incoming radiation via a rotating wire grid and flat mirror assembly. Each of the two polarizations can be directed into separate receivers. This arrangement allows either a

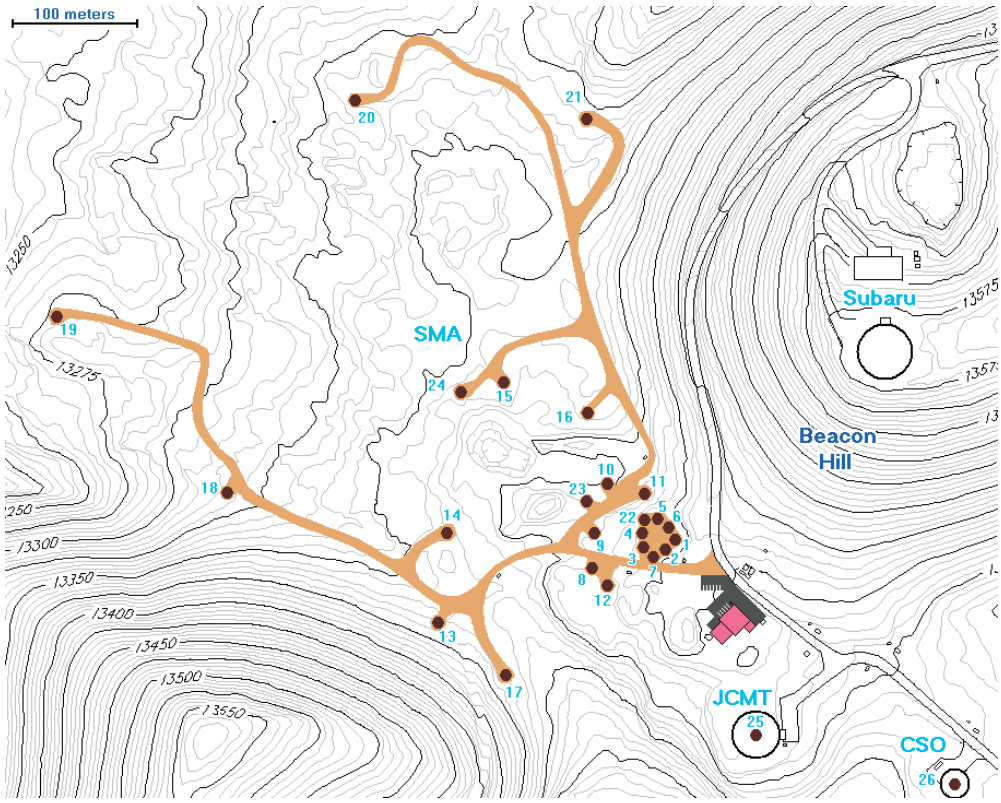

FIG. 3.—Twenty-four pads of the SMA are distributed in four nested rings. The design followed the Reuleaux triangle pattern as much as possible, as constrained by the site. E. Keto was responsible for optimizing the configuration. K. Young produced this diagram.

dual-polarization mode for maximum sensitivity or polarization measurements, or the simultaneous operation of a high-frequency and a low-frequency receiver. Optically injected local oscillator (LO) sources are also located above the receivers, while a calibration vane, as well as quarter wave plates, can be inserted into the optical path. The quarter wave plates provide circular polarization, but they have only been tested in the single receiver mode at 345 GHz.

Three receiver inserts that cover the 230, 345, and 690 GHz bands are now in operation. The hearts of these receivers are double-sideband mixers fabricated with niobium SIS junctions, which are cooled to 4.2 K along with the second-stage High-Electron Mobility Transistor amplifiers. On the SAO side, these junctions were fabricated by JPL. On the ASIAA side, a partnership with National Tsinghua University, Nobeyama Observatory, and the Purple Mountain Observatory produced the junctions (Shi et al. 2002). The instantaneous bandwidths of the receivers are 50, 100, and 60 GHz in the 230, 345, and 690 GHz bands, respectively. The double-sideband receiver temperatures in the laboratory setting were about 2, 2.5, and 7 times the quantum limit, or about 25, 35, and 200 K, respectively (Blundell 2004). The double-sideband receiver temperatures of the operational systems on the Array are currently about 80, 100, and 480 K, respectively. Technical descriptions of the receivers can be found in papers by Blundell et al. (1995) and Tong et al. (1996, 2003).

The phase-locked LO sources are based on Gunn Oscillators operating in the 100 GHz range, whose signals have been multiplied with diode doublers and triplers. For lower frequencies, the LO is injected into the optical path via a simple mesh grid. To achieve adequate power at 650 GHz, the LO is injected via a Martin-Puplett diplexer. The LO signals are coupled optically to the mixers from outside the cryostats.

Because of the large number of mechanical parts that must be tuned within the receivers, the goal is to have them under computer control to facilitate remote operation of the system and improve operational efficiency. The position of the wire grids and mirrors in the optical path, the calibration vane, the mechanically tuned LO, the mixers, and the phase-lock loops will all be put under servo control. Much of this capability is already in place for the lower frequency bands (Hunter et al. 2002).

On the telescopes, the receivers have worked quite well and were able to run for months and years at a time without failure. The cryostats must be warmed up periodically for coldhead maintenance (every 10,000 hr), but the junctions themselves are quite robust, despite repeated warming ups and cool downs due to power failures on site.

2.5. *Correlator*

The SMA correlator has a flexible hybrid analog-digital design. After the first down conversion, the intermediate-frequency (IF) band centered at 5 GHz from each receiver is broken up into six contiguous blocks of 328 MHz each, covering a total window of 2 GHz. Each block of 328 MHz, recentered at an IF of 1 GHz, is further split into four chunks of 104 MHz (82 MHz spacing). Thus, a total of 24 chunks or basebands are derived from each of two receivers for all eight telescopes. A maximum of 384 basebands are therefore presented to the digital part of the correlator, for a maximum of 1344 multilag cross-correlations. The digital part of the correlator consists of 90 boards, each with 32 custom-designed

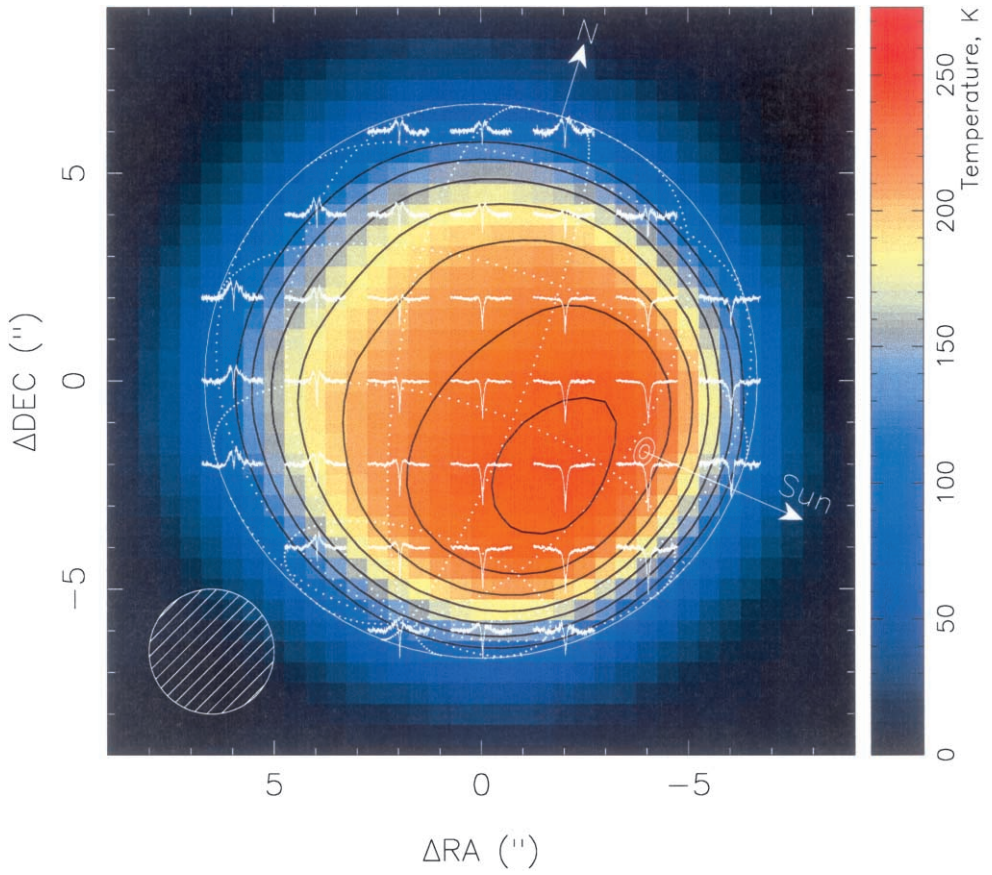

FIG. 4.—First image obtained with the full eight element array on 2003 November 12 of the 1.3 mm thermal surface emission and CO (2–1) atmospheric absorption from Mars at a spatial resolution of 3″. At the time of observations the apparent diameter of Mars was 13.″3. The absorption-line profiles are pressure broadened and can be used to infer the vertical distribution of CO and temperature in the atmosphere. This image was made by M. Gurwell.

correlator chips. These correlator boards were built by MIT-Haystack as part of the Mark IV correlator project (Whitney 2004). Hence, a minimum of two chips can be devoted to each baseband correlation. With 512 lags per correlator chip, a data rate demultiplex factor of 4 (the correlator clock rate is 52 MHz), and a factor of 2 for calculating both amplitude and phase, 128 spectral channels are obtained per baseband. Thus, if the full bandwidth is covered, a spectral resolution of 812.5 kHz is obtained. For full polarization measurements with all four stokes parameters, the spectral resolution would be a factor of 2 worse or 1.625 MHz. If fewer numbers of basebands are processed, more correlator chips can be used per baseband to achieve higher spectral resolutions. For example, if only one baseband per block is processed, 16 chips can be used on each baseband, achieving 101.6 kHz resolution. Furthermore, different basebands can be processed with different spectral resolutions, and the individual blocks can be tuned to different positions within the passband. By reprogramming the correlator boards to put more chips on a baseband, even higher spectral resolutions can be achieved.

When the SMA is linked to JCMT and CSO for joint interferometry beginning in 2005, the correlator will be able to process the full bandwidth on all 45 baselines with one receiver. Dual band capability could be achieved by reducing the number of baselines or bandwidth.

3. CALIBRATION OF THE INSTRUMENT

In order to operate the SMA as an interferometer, many system performance calibrations must be done. As previously described, the surfaces of the telescopes are set by holographic measurements, and the efficiencies of the telescopes are checked by observing planets and their satellites. The pointing models for the telescopes are determined first with data from optical guidescopes mounted behind holes in the primary reflectors (Patel 2000; Patel & Sridharan 2004). Typically, positions of more than 100 stars are measured throughout the sky, and 19-parameter pointing models are determined in order to correct for the collimation, tilt, sag, and encoder offsets. The residuals after the fit are typically 1″–2″ rms in each axis. While the pointing is stable on the order of days, there are long-term drifts in the tilt components of the telescopes, which might be associated with the stability of the antenna pads. After the optical pointing models have been determined, the alignment of the radio and optical axes of each telescope is checked by radio pointing on planets. During observations, pointing of the telescopes is verified and further improved by measurements of nearby strong continuum sources. Pointing measurements also can be made interferometrically by noding the antennas and analyzing the changes in fringe amplitude. The coordinates of the array elements are determined from the visibility phase measurements on strong quasars tracked over wide ranges of hour angle. Typically, the baseline data are taken at 230 GHz, and the antenna locations can be determined to an accuracy of 0.1–0.2 of a wavelength, or about 0.2 mm. Finally, the gain and phase of the array are tracked in real time by observing a nearby quasar interleaved with the program sources. Flux and passband calibrations are also done in standard fashion by observing planets.

Under optimal sky conditions, these calibration procedures may be sufficient. However, at higher frequencies and during poor weather conditions, auxiliary techniques will have to be implemented to correct for the gain and phase fluctuations. A number of different techniques are being considered, including self-calibration when the sources are strong enough and simple enough; calibration with respect to a maser source if the frequencies of the lines are nearby; cross calibration between different receivers utilizing quasars at lower frequencies or masers; and measuring phase fluctuations by monitoring the atmospheric water lines at 183 GHz (Wiedner et al. 2001) or 20 μm (Naylor et al. 2002) or the total power from the sky (Battat et al. 2004a, 2004b). These techniques, which will be important in the future for the operation of the Atacama Large Millimeter Array currently under construction in Chile, are also actively being developed by other groups (e.g., Welch 1999).

4. ARRAY PERFORMANCE

During the last 20 years, millimeter-wavelength interferometry has become a well-developed field (Sargent & Welch 1993), and the SMA will push this research to wavelengths shortward of 1 mm with angular resolution better than an arcsecond. While the array is just now being completed, early results show that (1) a surface accuracy of the telescopes of about 12 μm can be achieved, (2) the absolute pointing accuracy at the level of 2″ rms can be achieved by frequent monitoring of a nearby calibrator, (3) the receivers are sensitive and are operating at less than about 7 times the quantum limit on the telescopes, (4) the correlator works properly, and (5) amplitude and phase stability are good and are easily corrected with nearby calibrators on timescales of 30 minutes under favorable weather conditions. We have also learned that good weather with low opacity is a precious commodity that must be exploited effectively through the use of dynamic scheduling.

Figure 4 shows the first image made with all eight elements of the SMA operating at the $J = 2$–1 CO line of Mars. Comparisons of results from the SMA with other millimeter-wave interferometers such as the Institut de Radioastronomie Millimétrique, the Berkeley Illinois Maryland Association, the Owens Valley Radio Observatory, and the Nobeyama Millimeter Array at 230 GHz show that the images are consistent in terms of structures and intensities. The scientific potentials are illustrated by the results reported in the accompanying Letters. The abundance of spectral lines in the submillimeter window has been demonstrated by the observations of IRAS 18089−1732 (Beuther et al. 2004a, 2004c) and IRAS 16293−2422 (Kuan et al. 2004). The vertical abundance of CO and HCN in the atmosphere of Titan has been measured (Gurwell 2004). A circumbinary disk has been imaged in L1551 (Takakuwa et al. 2004). The nearest circumstellar disk in TW Hya has been imaged with about 100 AU resolution (Qi et al. 2004). The first 690 GHz interferometer maps were obtained toward IRC 10216 (Young et al. 2004). The first submillimeter wavelength image with subarcsecond resolution of the Orion KL region was obtained (Beuther et al. 2004b). High-velocity as well as low-velocity outflows have been detected in V Hya (Hirano et al. 2004). Polarized SiO maser features were imaged in VY Canis Majoris (Shinnaga et al. 2004). The ultracompact H II region G5.89 has been demonstrated to be the source of a molecular outflow imaged in the SiO line (Sollins et al. 2004). By surveying a number of other bright ultracompact H II regions, some have been found to be suitable calibrator sources (Su et al. 2004). Nearby galaxies M51 (Matsushita et al. 2004) and M83 (Sakamoto et al. 2004) have been imaged with small mosaic maps. Interacting galaxies have also been studied in the VV 114 system (Iono et al. 2004) and the NGC 6090 system (Wang et al. 2004).

We thank the Smithsonian Institution and the Academia Sinica for their support of this project. We thank the entire SMA team from SAO and ASIAA for their hard work over many years in making this instrument a reality. The most gratifying thanks are coming in the form of the exciting scientific results that this instrument is beginning to produce.

REFERENCES

Battat, J., Blundell, R., Hunter, T., Kimberk, R., Leiker, S., & Tong, C. 2004a, Proc. IEEE, in press
Battat, J., Blundell, R., Moran, J., & Paine, S. 2004b, ApJ, 616, L71
Beuther, H., et al. 2004a, ApJ, 616, L19
———. 2004b, ApJ, 616, L23
———. 2004c, ApJ, 616, L31
Blundell, R. 2004, in Proc. 15th Int. Symp. on Space Terahertz Technology, ed. G. Narayanan (New York: IEEE), in press
Blundell, R., et al. 1998, in Proc. 6th Int. Conf. on Terahertz Electronics, ed. P. Harrison (New York: IEEE), 246
———. 1995, Proc. IEEE, 43, 933
Gurwell, M. A. 2004, ApJ, 616, L7
Hirano, N., et al. 2004, ApJ, 616, L43
Hunter, T. R., Wilson, R. W., Kimberk, R., Leiker, P. S., & Christensen, R. 2002, Proc. SPIE, 4848, 206
Iono, D., Ho, P. T. P., Yun, M. S., Matsushita, S., Peck, A. B., & Sakamoto, K. 2004, ApJ, 616, L63
Keto, E. 1997, ApJ, 475, 843
Kuan, Y.-J., et al. 2004, ApJ, 616, L27
Masson, C. R. 1992, Design Study for the Submillimeter Interferometer Array (SAO Special Rep.; Harvard: SAO)
Matsushita, S., et al. 2004, ApJ, 616, L55
Moran, J. M., Elvis, M. S., Fazio, G. G., Ho, P. T. P., Myers, P. C., Reid, M. J., & Willner, S. P. 1984, A Submillimeter Wavelength Telescope Array: Scientific, Technical, and Strategic Issues (SAO Internal Rep.; Harvard: SAO)
Naylor, D. A., Gom, B. G., Schofield, I. S., Tompkins, G. J., & Chapman, I. M. 2002, Proc. SPIE, 4820, 902
Patel, N. A. 2000, Proc. SPIE, 4009, 88
Patel, N. A., & Sridharan, T. K. 2004, Proc. SPIE, 5496, 639
Qi, C., et al. 2004, ApJ, 616, L11
Raffin, P. 1991a, SMA Tech. Memo 51, http://www.cfa-sma.harvard.edu
———. 1991b, SMA Tech. Memo 55, http://www.cfa-sma.harvard.edu
Raffin, P., & Kusunoki, A. 1992, SMA Tech. Memo 59, http://www.cfa-sma.harvard.edu
Sakamoto, K., Matsushita, S., Peck, A. B., Wiedner, M. C., & Iono, D. 2004, ApJ, 616, L59
Sargent, A. I., & Welch, W. J. 1993, ARA&A, 31, 297
Shi, S. C., Wang, M. J., & Noguchi, T. 2002, Superconductor Sci. Tech., 15, 1717
Shinnaga, H., Moran, J. M., Young, K. H., & Ho, P. T. P. 2004, ApJ, 616, L47
Sollins, P., et al. 2004, ApJ, 616, L35
Sridharan, T. K., Saito, M., Patel, N. A., & Christensen, R. 2004, Proc. SPIE, 5495, 441
Su, Y.-N., et al. 2004, ApJ, 616, L39
Takakuwa, S., et al. 2004, ApJ, 616, L15
Tong, C., Blundell, R., Megerian, K., Stern, J., & LeDuc, H. 2003, in 13th Int. Symp. on Space Terahertz Technology (Harvard: SAO), 23
Tong, C., Blundell, R., Paine, S., Papa, C., Kawamura, J., Zhang, X., Stern, J., & LeDuc, H. 1996, Proc. IEEE, 44, 1548
Wang, J., et al. 2004, ApJ, 616, L67
Welch, W. J. 1999, in Reviews of Radio Science, ed. W. R. Stone (Oxford: Oxford Univ. Press), 787
Whitney, A. R. 2004, Radio Sci., 39, 1007
Wiedner, M. C., Hills, R. E., Carlstrom, J. E., & Lay, O. P. 2001, ApJ, 553, 1036
Young, K. H., et al. 2004, ApJ, 616, L51